

promoting access to White Rose research papers



Universities of Leeds, Sheffield and York
<http://eprints.whiterose.ac.uk/>

White Rose Research Online URL for this paper:
<http://eprints.whiterose.ac.uk/5398/>

Published conference paper

Allendes Osorio, R.S. and Brodlie, K.W. (2008) *Contouring with uncertainty*. In: Lim, Ik Soo and Tang, Wen, (eds.) *Theory and Practice of Computer Graphics 2008*. Proceedings. 6th Theory & Practice of Computer Graphics Conference (TP.CG.08) (UK Chapter of the Eurographics Association), 9 -11 June 2008, Manchester. Eurographics Association , pp. 59-66.

<http://dx.doi.org/10.2312/LocalChapterEvents/TPCG/TPCG08/059-065>

Contouring with Uncertainty

R. S. Allendes Osorio^{†1,2} and K. W. Brodlie¹

¹School of Computing, University of Leeds, United Kingdom

²Departamento de Computación, Facultad de Ingeniería, Universidad de Talca, Chile

Abstract

As stated by Johnson [Joh04], the visualization of uncertainty remains one of the major challenges for the visualization community. To achieve this, we need to understand and develop methods that allow us not only to consider uncertainty as an extra variable within the visualization process, but to treat it as an integral part. In this paper, we take contouring, one of the most widely used visualization techniques for two dimensional data, and focus on extending the concept of contouring to uncertainty. We develop special techniques for the visualization of uncertain contours. We illustrate the work through application to a case study in oceanography.

1. Introduction

One of the outstanding challenges in data visualization is the representation of uncertainty. All data is to an extent uncertain, whether it be due to simulation error or measurement error, but visualization techniques traditionally assume the data is exact and generate a picture accordingly. However there are an increasing number of application areas where uncertainty is a fundamental property of the data, and the integrity of the visualization is compromised unless the degree of uncertainty is made absolutely clear. This is true for example in ensemble computing where the underlying physical model is uncertain, and a range of simulations are carried out in order to get a broad view of the phenomenon. There is then no single ‘result’ but a set of possible results, each having its own probability of being ‘correct’. We need visualization techniques that can incorporate such uncertainty information. The issue is particularly pressing in view of the importance of some of the applications concerned. These include climate prediction studies where the correct handling of uncertainty information is vital in making decisions affecting the future of the planet.

In this paper we revisit one of the traditional visualization techniques, contouring, from the viewpoint of uncertainty. Normally we think of contouring as an operation on a grid of ‘exact’ data values, extracting lines along which the value

is estimated to be constant. But in uncertainty visualization we do not have scalar values at each grid point, but rather a Probability Density Function (PDF) of a random variable. For a random variable, Z , the PDF, f_Z , tells us that the probability that Z lies in the interval $[a, b]$ is given by:

$$\int_a^b f_Z(z) dz \quad (1)$$

Thus we suppose, at a given set of datapoints $(x_i, y_j), i = 1, 2, \dots, l, j = 1, 2, \dots, m$, we are given not scalar values z_{ij} , but random variables Z_{ij} defined by a PDF $F_{Z_{ij}}(z)$. Common PDFs would include Gaussian distributions where the errors are assumed to be normally distributed about the mean, and uniform or rectangular, where the probability of Z is assumed to be evenly spread within an interval.

How do we extend the concept of contour drawing to such data? The conventional approach, with exact data, is based on a vector approach (to an extent inherited from early graphics technology which itself was line-based). Intersections of contours with the grid lines are computed, and the intersection points joined up to provide an estimate of the contours themselves. This joining up of intersections can be seen as an approximation to the contour line of the bilinear interpolant within each grid cell, but for widely spaced grids this approximation can be poor, and care is needed to handle ambiguities when each pair of opposite vertices of the cell are both above, and both below, the contour value [LB98]. As well as contour line drawing, contour area drawing is also a common visualization technique, where the area in

[†] scrsao@leeds.ac.uk

which the data is estimated to lie between two given values is drawn. Again this is typically drawn as a vector-based approach, with the polygonal areas between successive contour lines being shaded in a particular colour representing the range of values covered.

To handle uncertainty, we take a raster-based approach. For any pixel, we shall compare its value with the value of the contour - remembering that the value at a pixel is not a single scalar, but rather a random variable with associated PDF. We derive analogues to both contour line drawing, and contour area drawing.

Our driving application comes from oceanography. The ocean dynamic topography, defined as the height of the sea surface above its rest state (the geoid), allows scientists to study the absolute circulation of the ocean and associated currents that help regulate the earth's climate. But determining this topography is a particular challenge, and different models predict different topographies. Bingham and Haines [BH06] use an ensemble of eight models to determine a composite 'Mean Dynamic Topography', and we use their results as our case study. Note that for the North Atlantic the composite MDT has values ranging between -50 and +50cm, but the RMS error is significant - of the order of 3.2cm. This large uncertainty needs to be incorporated within the visualization, otherwise false conclusions might be drawn.

Section 2 reviews a range of previous work on uncertainty visualization. Section 3 explores how the notion of interpolation, fundamental in allowing us to create an overall model from the data, carries over to the uncertainty situation, and goes on to consider the meaning of a contour in this context. This work underpins section 4 where we look at different ways of representing contours with uncertainty, using the oceanography case study to illustrate the different techniques. Finally section 5 presents conclusions and discusses how the work can be extended to isosurfacing of 3D data.

2. Background and Related Work

There is a growing awareness of the importance of uncertainty in scientific visualization. Johnson [Joh04] selects the representation of error and uncertainty as one of his top scientific research problems. He makes the point: 'when was the last time you saw an isosurface with error bars?', contrasting this with the presentation of 1D graphs in science and engineering journals where error bars are common.

A good description on uncertainty visualization specifically applied to geographical data, including the challenges that need to be addressed to achieve appropriate representations, is presented by MacEachren et al. [MRH*05]. Uncertainty visualization has also been studied in a series of papers by Pang, Kao and their colleagues. A good review of the present state of the art can be found in the paper by Love, Pang and Kao [LPK05]. We focus in this section on

papers which relate to contouring and the related problem of isosurfacing.

Rhodes et al [RLBS03] address uncertainty in isosurface rendering, from a viewpoint of multiresolution modelling. At coarse resolution, errors are defined at each datapoint. These are interpolated to give error values at the vertices of the isosurface triangular mesh, and the error values are mapped to visual cues such as colour. Thus the isosurface of the 'mean' values is drawn, but coloured with an indication of the error values at nearby datapoints. This could translate easily to contour drawing, by drawing the contour line of the 'mean' data values, colouring the line with an indication of the error. The disadvantage of this approach is that it does not give any clear indication of the range of possible locations of the contour line (or isosurface).

Bingham and Haines [BH06] in their ocean dynamic topography paper include an indication of uncertainty. Contour lines are used to visualize the height of the composite MDT, and this is overlaid on top of an 'error image': this image shows the error field for the composite MDT. However this has precisely the same disadvantage as that of Rhodes et al: the errors relate to the uncertainty of the data values, not the visualization (i.e. location of contour line).

Love et al [LPK05] consider the visualization of multi-value data, as is the case with our ocean dynamic topography data and indeed many other climate simulation studies. They infer a PDF at each grid point from the multivalued data, as we shall do. They define an interpolation operator which constructs a PDF along the grid line between datapoints. This allows them to search for the best match against a target PDF which describes the expected behaviour of the contour value. This gives intersection points along grid lines, which can be connected as in conventional contouring. They suggest exactly the same approach for isosurfacing: they match the interpolated PDF along each grid line against a target PDF in order to get the intersection points, and then pass these to a standard marching cubes algorithm. Once again the uncertainty in the location of the contour line or isosurface is not visible in the visualization that is produced.

3. Modelling Uncertain Data

3.1. Interpolation

In visualization we typically begin by creating, from the given data, an empirical model of the underlying phenomenon from which our data has been sampled. This is very often achieved by interpolation. This is exactly the approach we follow here.

We begin by considering interpolation in one dimension, in the unit interval $[0, 1]$. Suppose we have a random variable Y_1 , with PDF $f_{Y_1}(y)$, at $x = 0$, and another random variable Y_2 , with PDF $f_{Y_2}(y)$, at $x = 1$. We are interested in the PDF of a random variable, W , which is a linear combination of Y_1

and Y_2 , say:

$$W = c_1 Y_1 + c_2 Y_2 \quad (2)$$

Fortunately the derivation of the resulting PDF for the two types of distribution we are interested in for uncertainty visualization, Gaussian and uniform, is well known (see, for example, [CH04]). For our case study, we need the result for the Gaussian case, and the details are as follows.

Suppose Y_1 and Y_2 are Gaussian distributions with means μ_1 and μ_2 , and standard deviations σ_1 and σ_2 . Then the random variable W has a Gaussian distribution with mean μ_W given by:

$$\mu_W = c_1 \mu_1 + c_2 \mu_2, \quad (3)$$

and standard deviation σ_W given by:

$$\sigma_W = (c_1^2 \sigma_1^2 + c_2^2 \sigma_2^2)^{\frac{1}{2}}. \quad (4)$$

For interpolation at point α in the unit interval, we take $c_1 = (1 - \alpha)$ and $c_2 = \alpha$. Note that whereas the mean is a linear combination of the individual means, the variance is a *nonlinear* combination of the individual variances. Thus we are able to estimate the PDF at any point along the grid line between two datapoints.

For contouring, we need 2D interpolation and this proceeds in a similar way. Consider now a unit square, with Gaussian random variables defined at each vertex, say $Z_{00}, Z_{10}, Z_{11}, Z_{01}$, in an obvious notation. At the interior point (α, β) , the random variable $Z_{\alpha\beta}$ defined as:

$$Z_{\alpha\beta} = (1 - \alpha)(1 - \beta)Z_{00} + \alpha(1 - \beta)Z_{01} + (1 - \alpha)\beta Z_{10} + \alpha\beta Z_{11} \quad (5)$$

has a Gaussian distribution with mean $\mu_{\alpha\beta}$ given by:

$$\mu_{\alpha\beta} = (1 - \alpha)(1 - \beta)\mu_{00} + \alpha(1 - \beta)\mu_{01} + (1 - \alpha)\beta\mu_{10} + \alpha\beta\mu_{11} \quad (6)$$

and standard deviation $\sigma_{\alpha\beta}$ given by:

$$\sigma_{\alpha\beta} = ((1 - \alpha)^2(1 - \beta)^2\sigma_{00}^2 + \alpha^2(1 - \beta)^2\sigma_{01}^2 + (1 - \alpha)^2\beta^2\sigma_{10}^2 + \alpha^2\beta^2\sigma_{11}^2)^{\frac{1}{2}}. \quad (7)$$

This result follows by repeated application of the result for the 1D case in the paragraph above.

Finally we can apply the above result in each grid square of our 2D mesh, giving us a piecewise bilinear interpolation of the PDFs.

3.2. Defining a Contour

From data expressed as PDFs at the points on our grid, we are now able to calculate the PDF of the random variable at any interior point. How do we define a ‘contour’ in this uncertainty context?

In the traditional case with exact values, for a function z , we can define a contour of iso-value h as the set of points (x, y) , such that:

$$\{(x, y) : z(x, y) = h\}. \quad (8)$$

We need a new definition in the uncertain case because there is no notion of a random variable having an exact value, h . Instead we are interested in the probability that Z has a value ‘close’ to h . Clearly we move from having precise contour *lines* of value h , to *areas* where we deem the probability of the random variable at (x, y) being close to h is sufficient for it to be highlighted in some way. We need to be concerned with what we mean by ‘close to’, and ‘sufficient’. We begin by defining a property associated with each point of the domain, and call this the *contour probability* - it is a function Q of the point (x, y) , the contour value h , and a parameter ϵ . We define the contour probability in mathematical notation as:

$$Q(x, y; h; \epsilon) = Pr(|Z(x, y) - h| \leq \epsilon) \quad (9)$$

Descriptively, the contour probability measures the probability that the random variable Z at (x, y) takes a value within ϵ of h . That is, it gives some meaning to the expression ‘close to’.

We are now able to extend the notion of contouring to the context of uncertainty. In mathematical terms, we are interested in the points (x, y) where:

$$Pr(|Z(x, y) - h| \leq \epsilon) \geq \theta \quad (10)$$

that is,

$$Q(x, y; h; \epsilon) \geq \theta, \quad (11)$$

for some values of ϵ and θ . We can define this set of points as the *uncertain contour* of threshold h . In descriptive terms, we are defining the uncertain contour as the set of points where the contour probability is greater than some level θ , that is, the probability that the random variable Z at (x, y) takes a value within ϵ of the contour value, is greater than θ . This gives some meaning to ‘sufficient’.

4. Results

4.1. Case-Study: Oceanography

As mentioned before, an Ocean Dynamic Topography (ODT), defined by Bingham and Haines in [BH06] as “the height of the sea surface above its rest-state (the geoid)”, is of relevance to oceanographers when studying the absolute circulation of the ocean, which in turn helps them determine the surface currents involved in regulating the earth’s climate.

However, difficulties in getting reliable measurements of the dynamic topography, mainly due to the limitations in the determination of the geoid, mean that scientists have to use

alternate methods, such as the calculation of mean dynamic topographies (MDT), which represents the time-dependent part of the dynamic topography, allowing them to remove the geoid from the calculations [BH06].

Bingham and Haines [BH06] propose a new approach to obtain a composite MDT by combining a number of MDTs and converting the spread amongst them into a formal error estimate. Having calculated this composite MDT, it is of importance for the authors to display both the values and the estimated error.

Working in collaboration with the University of Reading, it was possible to obtain the eight original models used in the original derivation of the composite MDT. These models are each described on a two-dimensional regular grid over the North Atlantic, in which the coordinates of the lowest-left grid point in degrees are 41N 79W, and of the upper-right are 77N 13E, and where the height is measured in centimetres. The spacing between grid points is equivalent to 1/9 degrees in both latitude and longitude, which results in a 829 by 325 grid.

Having this data, it was possible for us to do our own derivation of a composite model, which integrates the information of the original models and, at the same time, includes an estimate of the error included in the calculation.

To derive our MDT, we averaged the values from the eight original models at each point in the grid to obtain a sample mean. In addition to this, we can calculate the standard deviation of the sample, which is given by the following relation:

$$s = \sqrt{\frac{1}{n-1} \sum_{k=1}^n (z_k - \bar{z})^2} \quad (12)$$

where z_k is the value at the current vertex for the k -th original MDT; \bar{z} is the mean value, obtained from all MDT's at the current vertex; and $n = 8$ is the number of available MDTs.

Using the mean and the standard deviation statistics, and assuming a Gaussian distribution, we can generate our composite MDT grid, of the same size as the original MDTs and where each vertex has a random variable Z with PDF in the form $N(\mu, \sigma)$ with $\mu = \bar{z}$ and $\sigma = s$.

Figure 1 shows the mean values of our composite MDT. It is clear from the image that the data is defined over the North Atlantic area. Known landmasses such as the British Isles (lower right corner) and Canada (left side) are also clearly recognizable despite the low resolution derived from the several different original sampling techniques. An HSV colour scale has been used to map valid data values, whilst black is used to depict *no data* values.

4.2. 'Line' methods

In Section 3.2 we presented a definition of uncertain contours as the group of points where the probability that the

random variable is 'close' to the contour value exceeds a constant. We need now to find ways in which this description can be translated to a visual format.

Uncertainty bands

From Equation 10, it is clear that, any pixel in the final image will either satisfy or not the condition of having probability above a preselected value θ . Having a boolean type of output, it is quite simple and straightforward to map this to intensity as follows:

$$I(x,y) = \begin{cases} 1 & \text{if } Pr(|Z(x,y) - h| \leq \epsilon) \geq \theta \\ 0 & \text{otherwise} \end{cases} \quad (13)$$

where θ represents the constant selected for the probability.

As expected, the visual result of this operation is seen as a band, or a two-dimensional contour (having a finite width), which contrasts with the more usual one-dimensional contours.

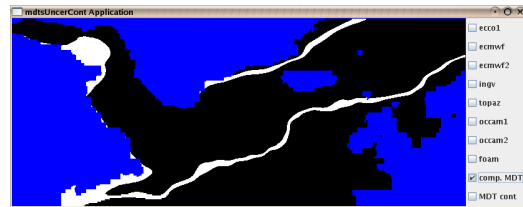


Figure 2: Zero band for the composite mdt dataset.

The zero contour, $h = 0$, is of particular interest. Figure 2 shows the application of such a method for the calculation of a 'zero-band' in the composite MDT dataset. In our experience, a distance from the contour value of $\epsilon = \sigma$ with a probability $\theta = 0.65$ is useful, and thus was used to produce the image. In other words, each pixel highlighted in the image indicates that there is a 65% or greater probability of the pixel having value close enough to the contour value, and thus, satisfying the equation $Pr(|Z(x,y) - h| \leq \sigma) \geq 0.65$, for $h = 0$.

Fuzzy contours

In the previous method, we used the *contour probability* function Q , defined in section 3.2 to visually identify points in the domain with value close enough to a specific contour.

The next obvious step is to identify how close in value the pixels are to a given contour value. Again, by looking at Equation 9, we see that because function Q is described as a probability, it can be used directly as a measure of the closeness of a point to a given contour.

Probability values can therefore be mapped directly to intensity as follows:

$$I(x,y) \propto Q(x,y;h,\epsilon) = Pr(|Z(x,y) - h| \leq \epsilon) \quad (14)$$

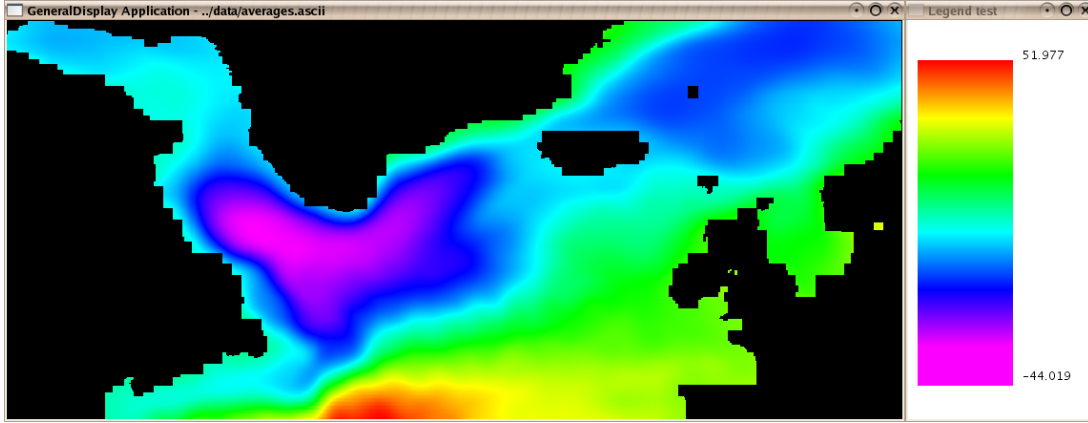


Figure 1: Colour map of the mean values (height) at each pixel for the composite MDT dataset.

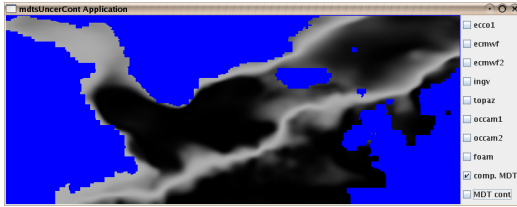


Figure 3: A fuzzy zero contour for the composite MDT dataset.

Figure 3 shows the result of calculating a zero-contour for the composite MDT dataset using this method. Again, a value $\epsilon = \sigma$ was chosen to identify pixels in the image close to the zero-contour, however, it is also clear from the intensities in the image that the degree of closeness varies between pixels.

4.3. 'Area' methods

A usual extension for contouring algorithms is to use colour to shade the areas that lie in between contour lines [SML98]. After looking into ways in which traditional contour lines can be extended to include uncertainty notions, we will now look into how the idea of colour shading can also be extended to the case where each vertex in the grid has a PDF rather than a scalar value.

In the simplest case of just one zero-contour, if we consider that PDFs are continuous functions defined in the range $(-\infty, \infty)$, then the zero-contour would divide the whole range into two regions $R_1 = (-\infty, 0)$ and $R_2 = [0, \infty)$. And the probability of each point in the domain to be on each of these regions is given by the integral of the PDF between the limits of each range.

If we want to generalise this to N contours and $N + 1$ re-

gions, and recalling the definition given in Equation 1, we can see this would imply the calculation of the following probabilities

$$Pr(Z(x,y) \in R_i) = \int_{h_{i-1}}^{h_i} f(x,y;z) dz \quad \forall i = 1 \dots (N+1) \quad (15)$$

where $h_0 = -\infty$, $h_{N+1} = \infty$ and $h_i; i = 1 \dots N$ are the N contours.

Uncertain banded areas

A first way of shading areas whilst considering the uncertainty can be derived directly from the uncertain bands method introduced earlier. By selecting an appropriate value $\theta > 0.5$, and comparing it with probabilities calculated according to Equation 15, then for each point in the domain it is possible to say whether it has some certainty (probability greater than θ) of belonging to one particular region, or whether it is impossible to make any definite assignment.

Thus, areas can be shaded according to the following

$$C(x,y) = \begin{cases} c_i & \text{if } Pr(h_{i-1} \leq Z(x,y) \leq h_i) > \theta \\ 0 & \text{(background) otherwise} \end{cases} \quad (16)$$

where c_i represents the base colour for the i -th section.

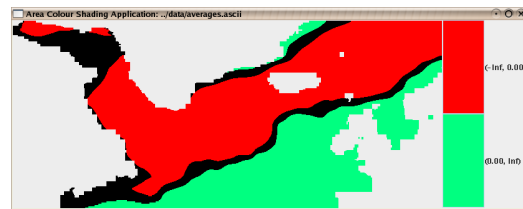


Figure 4: Colour coding of two distinct areas according to a value of $\theta = 0.65$.

Figure 4 shows the application of this method to the composite MDT dataset considering only the basic zero-contour,

thus dividing the whole range over which PDFs are defined in only two distinctive, non-overlapping sections, and using a value of $\theta = 0.65$.

For the previous example, black has been selected as background colour. Also clear from Figure 4 are the areas where, according to Equation 16, background color has been applied, i.e. points where we can not be sure with a probability greater than θ , to which region the point should belong.

Fuzzy areas

As a second step in the colour shading of areas, and also extending from the idea of fuzzy contours presented earlier, if we discard the idea of a limit θ and simply blend the base colours according to the probabilities calculated from Equation 15, it is possible to achieve the effect of having a fuzzy boundary between the differently shaded areas.

There are multiple ways in which we can achieve the blending of base colours. In particular, we have experimented with linear combination of colours and the use of transparency. We will describe both approaches using the same general frame of having a series of $N + 1$ different, non-overlapping sections, and the corresponding N contour levels ($h_1 \dots h_N$), and having $h_0 = -\infty$ and $h_{N+1} = \infty$.

Firstly, if we think of the blending process as the linear combination of base colours, then we can use the probabilities from Equation 15 as weighting factors. Using this approach, the final colour for each point is obtained with the following relation

$$C(x, y) = \sum_{i=1}^{N+1} c_i * Pr(h_{i-1} \leq Z(x, y) \leq h_i) \quad (17)$$

where $C(x, y)$ represents the final colour at each point and c_i represents the colour used to shade the i -th section.

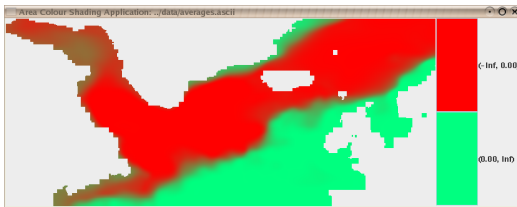


Figure 5: Colour coding of two distinct areas using a fuzzy boundary.

Figure 5 shows the results of using a weighted sum of colours (in this particular case red for values below zero and green for those above it) to represent two different sections within the composite MDT dataset. Notice that, as expected from the results shown so far, the boundary between the two areas does indicate the mixture of both original colours.

A second way to achieve the blending of colours is by using transparency. To implement such a method, we first

need to select a background colour, on top of which successive semi-transparent layers, one for each of the individual sections, are painted. The transparency value for each section is taken as the probability.

Random areas

In general, PDFs can be taken as input for random generating number algorithms. In our case, by generating random numbers based in the PDFs at each vertex of a grid, we create a random instance of the original data. And, because this new instance is made of scalar values, traditional visualization techniques, such as a normal region based shading, can be used to visualize them.

Even though we have reduced the information when creating an instance from a whole PDF to a single scalar value, uncertainty would still be shown by a normal colour shading algorithm. This is because each pixel is individually assigned to a particular colour. Then because of the random nature of the data values generated, the classification of points close to the contour will tend to vary greatly in comparison to those further away from it, thus translating into visual cues of uncertainty.

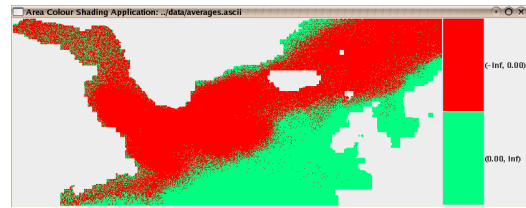


Figure 6: Snapshot showing colouring of pixels according to the value randomly generated from the original PDFs.

Figure 6 shows the result of using a normal shading approach to depict a zero-contour in a randomly generated instance of the composite MDT dataset. In the image, areas with larger number of points classified to different sections show the uncertainty in the boundary between sections.

Additionally, by generating a sequence of random instances, using a normal colour shading algorithm on each of them, and animating them through time, it is possible to increase the number of cues regarding the uncertainty in the location of the border between areas. Such an application will show a larger number of variations in the colour the same point is classified through different instances, whilst showing a constant colour in those areas where the classification is less uncertain.

5. Conclusions and Future Work

In this paper we have extended the traditional notion of contouring to the situation where the given data is accompanied by an uncertainty measurement. We have developed a variety

of methods which can be used to incorporate an uncertainty component into a contour-type visualization. In contrast to other approaches, we have aimed to give an indication of the different locations a contour line might have. The work has been illustrated through its application to a case study in oceanography, of importance to climate change studies.

Our approach in this paper has been pixel-based: that is, we compare each pixel value against the contour value. This is more computationally demanding than the more traditional vector-based approaches, but is well within the capability of modern processors. However we are also interested in extending vector-based methods to the uncertainty case, and in comparing the results with the pixel-based approach here.

The concepts developed in this paper will extend to 3D datasets, giving us an approach to isosurfacing of uncertain data. We can use the same methods as in this paper to determine the probability that a particular voxel has value sufficiently close to an isosurface value, as we used to determine the closeness of a pixel value to a contour value. We aim to report on this in a later paper.

6. Acknowledgements

We would like to acknowledge the help provided by Dr Rory Bingham and Professor Keith Haines at the University of Reading in terms of providing the dataset used as case study for this report and for their help in reviewing our work and suggesting a number of improvements.

We would also like to thank Professor David Duce, who suggested the idea of using transparency.

Finally we would also like to thank Dr Adriano Lopes, who helped formulate many of the issues we have addressed in this paper, and helped us in our initial thinking.

References

- [BH06] BINGHAM R. J., HAINES K.: Mead dynamic topography: intercomparisons and errors. *Philosophical Transactions of The Royal Society A* (2006), 903 – 916.
- [CH04] COX M., HARRIS P.: *Uncertainty Evaluation*. Tech. rep., National Physical Laboratory, March 2004. Software Support for Metrology. Best Practice Guide No. 6.
- [Joh04] JOHNSON C.: Top scientific visualization research problems. *IEEE Computer Graphics and Applications* (July/August 2004), 13–17.
- [LB98] LOPES A., BRODLIE K.: Accuracy in contour drawing. In *Proceedings of Eurographics* (1998), pp. 301–312.
- [LPK05] LOVE A. L., PANG A. T., KAO D. L.: Visualizing spatial multivalued data. *IEEE Computer Graphics and Applications* (2005), 69–79.
- [MRH*05] MACEACHREN A. M., ROBINSON A., HOPPER S., GARDNER S., MURRAY R., GAHEGAN M., HETZLER E.: Visualizing geospatial information uncertainty: What we know and what we need to know. *Cartography and Geographic Information Science* 32, 3 (July 2005), 139–160.
- [RLBS03] RHODES P. J., LARAMEE R. S., BERGERON R. D., SPARR T. M.: Uncertainty visualization methods in isosurface rendering. In *Proceedings of Eurographics* (2003), Chover M., Hagen H., Tost D., (Eds.), The Eurographics Association.
- [SML98] SCHROEDER W., MARTIN K., LORENSSEN B.: *The Visualization Toolkit*. Prentice Hall, 1998.